communications biology

Article

https://doi.org/10.1038/s42003-024-07097-2

# Sulfated galactofucan from *Sargassum fusiforme* protects against postmenopausal osteoporosis by regulating bone remodeling



Bao Yizhong [1,4], Fen Chen[2,4], Weihua Jin[2], Jihua Dai[1], Genxiang Mao[1] ✉ & Boshan Song[3] ✉

Osteoporosis is a degenerative bone disease highly prevalent in older women, causing high morbidity and mortality rates. Fourteen kinds of fucoidan were isolated from *Sargassum fusiforme* through acid (named as SFS), alkaline (SFJ) and water (SFW). SFW was passed through an anion exchange column to obtain SFW-0, SFW-0.5 and SFW-2. SFW-0.5 and SFW-2 were degraded to obtain different sulfate group contents SFW-x-M/S/O (x for 0.5 or 2). We further confirmed SFW-0.5-O was the most effective fraction of SFW. SFW-0.5-O may have alternating backbones of (Gal)n and (Fuc)n, and the main sulfation may be at C2/C3 of the Fuc/Gal residues. SFW-0.5-O inhibition of OC differentiation was associated with IRF-8 signaling; meanwhile, SFW-0.5-O promoted osteoblast differentiation and bone mineral nodule formation. SFW-0.5-O also effectively ameliorated osteoporosis symptom caused by estrogen deprivation in vivo. We uncovered that the fucoidan active fraction SFW-0.5-O demonstrated effective bone protection, may be exploited for osteoporosis therapy.

Osteoporosis(OP) is a systemic skeletal disorder characterized by reduced bone mass, deteriorated skeletal microarchitecture and caused by dysregulated bone metabolism[1]. Postmenopausal osteoporosis (PMOP) is the major type of primary OP associated with the apparent degradation of bone structural integrity due to estrogen deficiency[2]. PMOP increases susceptibility to fragility fractures, thus contributing to disability and mortality[3], dramatically reducing patients' quality of life, and causing a heavy public burden[4]. Drug therapy is the primary clinical treatment for OP, including anti-resorptive drugs such as bisphosphonates and denosumab[5], of which the main pharmacological effect is the inhibition of osteoclast(OC) activity; however, long-term treatment with these anti-resorptive drugs can cause serious adverse effects, such as bisphosphonate-associated musculoskeletal pain, osteonecrosis of the jaw and atypical femur fractures[6]. Furthermore, pharmacological promotion of osteoblast(OB) differentiation is still lacking due to a limited understanding of the molecular mechanisms governing osteogenesis[7]. Hence, the medical dilemma and financial burden of OP highlight the urgent need to develop new approaches for the prevention and treatment of OP.

The bone remodeling process, focusing on bone resorption by OCs and bone formation by OBs, poses a significant concern in the treatment of OP[8]. Inhibition of osteoclastogenesis is an important strategy for preventing and treating OP[9]. The nuclear factor-κB (NF-κB) receptor activator ligand (RANKL) regulates OC differentiation and function. RANKL binds to its receptor RANK and initiates intracellular downstream signaling pathways to promote OC differentiation and bone resorption[10]. Interferon regulatory factor 8 (IRF-8) controls the monocyte/macrophage development[11], which is derived from myeloid progenitor cells in bone marrow[12], having a negative regulatory role in the process of osteoclastogenesis[13]. Down-regulation of IRF-8 negatively regulates NFATc1 and triggers an increase in osteoclastogenesis and activity[14], leading to disorders of bone metabolism and the development of OP[15]. Oligosaccharides from *Sargassum thunbergii* can inhibit OC differentiation by upregulating IRF-8 levels[16]. On the other hand, mature OBs are located near the newly synthesized bone matrix and produce the bone mineral hydroxyapatite, deposited in the organic matrix to form a dense bone mineralized matrix[17]. Accordingly, promoting OB differentiation is also a feasible way to treat OP. Fucoidan stimulates osteogenic differentiation of periodontal ligament stem cells[18] and human mesenchymal stem cells[19].

Fucoidan (SF) is a sulfated polysaccharide isolated from seaweeds[20,21]. Although some SFs do not exhibit pro-osteogenesis effects due to species

[1]Zhejiang Key Laboratory of Geriatrics and Geriatrics Institute of Zhejiang Province, Zhejiang Hospital, Hangzhou, PR China. [2]College of Biotechnology and Bioengineering, Zhejiang University of Technology, Hangzhou, PR China. [3]Department of Orthopaedic Surgery, Zhejiang Hospital, Hangzhou, PR China. [4]These authors contributed equally: Bao Yizhong, Fen Chen. ✉e-mail: maogenxiang@163.com; 735395261@qq.com

and molecular weight dependency[22], most SFs have been reported to exert an anti-bone resorption effect and promote bone formation. Regarding bone resorption, SF blocks RANKL-stimulated osteoclastogenesis and bone loss by modulating the Akt/NFATc1 signaling pathway[23] and NF-κB signaling[24]. Regarding osteogenic potential, low molecular weight fucoidan (LMWF) which has advantages in solubility and cellular uptake can promote OB proliferation in vitro, characterized by an increase in the outcome cell markers ALP and type 1 collagen[25]. Pereira et al. [26]. also demonstrated in vitro potential of SF to promote osteogenic differentiation and increase calcium deposition. In vivo, LMWF has been shown to increase femoral mineral density and significantly improve ovariectomy-induced bone microarchitectural degeneration in Sprague-Dawley rats[27]. It can also increase bone mineral salt density and ash weight in ovariectomized mice[28]. The byproduct of polysaccharide-enriched *Hizikia fusiforme* processing has osteoprotective effects; yet, this study only reported the effect of crude polysaccharides, while the kinds, molecular weight and the main active components of SF have not been elucidated.

Due to the structural diversity of SF, we investigated the anti-OC differentiation ability of SF extracted from *Sargassum fusiforme* and further degraded, isolated, and purified the obtained components to explore the effect of structure on the activity of SF and identify the best active component by structure-activity relationship analysis. Next, we extensively evaluated the role of SF active ingredients in inhibiting OC differentiation and promoting OB mineralization in vitro, and carried out in vivo experiments to investigate its roles and mechanisms in ameliorating bone degeneration in ovariectomized (OVX) mice, by which comprehensively assessed its anti-osteoporotic utility.

## Results

### Effect of extraction method of fucidans on osteoclastogenesis

To investigate the inhibitory effect of SFs extracted from *Sargassum fusiforme* by different extraction methods (acid extraction, alkaline extraction, and hot water extraction, Fig. 1A) on OC differentiation, we used TRAP staining assay to examine the differentiation of OCs, qPCR, and Western blot to verify the mRNA level and protein level during differentiation. First, an MTT assay was used to detect the cytotoxicity of SFs, detecting no significant cytotoxicity at a dose of 10 μg/mL for 48 h (Supplementary Fig. 1). As shown in Fig. 1B, C, TRAP staining revealed that 10 μg/mL SFW had better inhibition of OC differentiation compared to SFJ and SFS, up to more than 90% vs PBS. qPCR was then performed to assess the influence of

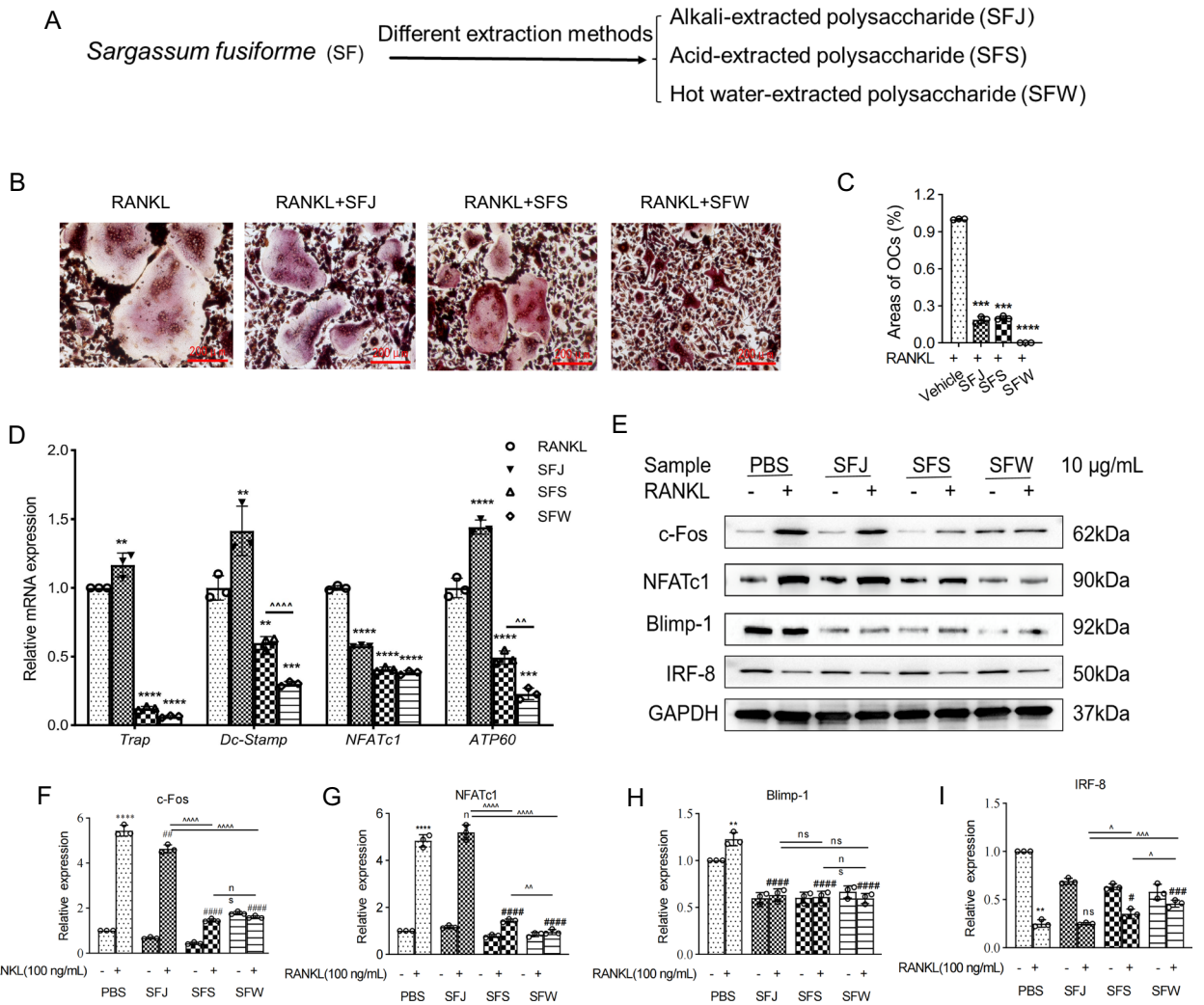


**Fig. 1 | Suppression of osteoclast differentiation by SF obtained from three extraction methods. A** Fucoidan (SFS, SFJ, SFW) were extracted by acid extraction (0.1 M HCl), alkali extraction (5% $Na_2CO_3$), and hot water extraction from Sargassum fusiforme. **B** TRAP staining of RAW264.7 was conducted following culture for 5 days with RANKL (50 ng/mL), and appropriate SFS, SFJ, SFW (10 μg/mL). **C** TRAP-positive cell area was quantified by Image J, Scale bar = 200 μm. **D** RT-qPCR was used to assess the expression of genes (*Trap, DC-Stamp, NFATc1, ATP60*) related to osteoclastic differentiation. RAW264.7 cells were treated with RANKL (100 ng/mL) and SFS, SFJ, SFW at a concentration of 10 μg/mL for 3 days. **E** Effect of SFS, SFJ, SFW on the expression levels of c-Fos, NFATc1, Blimp-1 and IRF-8. **F–I** The semi-quantitative analyses were conducted by Image J. Data are expressed as mean ± SD, n = 3. $^{*}P < 0.05$, $^{**}P < 0.01$ and $^{***}P < 0.001$ *vs.* CTRL; $^{\#}P < 0.05$, $^{\#\#}P < 0.01$ and $^{\#\#\#}P < 0.001$ *vs.* RANKL, $^{\wedge}P < 0.05$, $^{\wedge\wedge}P < 0.01$ and $^{\wedge\wedge\wedge}P < 0.001$ compared with other extraction methods.

SFs on OC-specific gene, including *Trap, NFATc1, ATP60*, and *DC-Stamp*. 10 μg/mL SFS and SFW caused a significant down-regulation in the transcription of these osteoclastogenesis-related genes after 3 days of RANKL action vs PBS control, while SFJ did not show a significant suppression effect (Fig. 1D).

IRF-8 signaling has been demonstrated to regulate osteoclastogenesis negatively[13]. Since SFs can effectively inhibit OC differentiation, we investigated the effect of 10 μg/mL SFs on the IRF-8/NFATc1 signaling pathway in vitro after 24 h. As shown in Fig. 1E–G, the expression of c-Fos and NFATc1, which promote OC differentiation, increased up to five times after RANKL treatment. The expression of IRF-8 decreased roughly 20%, while the expression of Blimp-1, which serves as an IRF-8 inhibitory subunit, increased (Fig. 1E, H, I). The above protein phenotypes due to RANKL were abrogated by the SFS and SFW administration, supporting that SFS and SFW upregulate the IRF-8 signaling. Among them, the upregulation of IRF-8 by SFW was one times more than SFS (Fig. 1I). Meanwhile, SFJ obtained by alkaline extraction did not effectively suppress the activity of OCs, so we chose the SFW obtained by water extraction for the subsequent experiments.

### Effect of different carbohydrate content and sulfation degree components on the ability of SFW to inhibit OC differentiation

In order to investigate the inhibitory effect of different carbohydrate fractions and sulfated SFW fractions on OC differentiation, SFW was purified into anion-exchange columns to obtain different graded fractions (SFW-0, SFW-0.5, SFW-2, Fig. 2A). The results of TRAP staining are shown in Fig. 2B, C. Compared to SFW-0 and SFW-2, the effect of 10 μg/mL SFW-0.5 reduced the number and size occupied by OCs in the field of view over 95% vs PBS after 5 days of RANKL induction. qPCR further showed that the expression of OC-related genes was suppressed after 10 μg/mL SFW-0.5 treatment compared to the RANKL group, while SFW-0 and SFW-2 treatment did not down-regulate the expression of these genes (Fig. 2D). Therefore, SFW-0.5 resulted as the effective component of SFW to suppress OC.

### Anti-osteoclast differentiation ability of SFW-0.5 and SFW-2

To investigate whether the molecular weight affects the anti-OC differentiation activity of SFs, hydrogen peroxide was used to degrade the 0.5 M eluted fraction oxidatively (SFW-0.5) and 2 M eluted fraction (SFW-2) to obtain SFW-0.5-L and SFW-2-L (Fig. 2E) respectively, which had only a change in molecular weight due to the breaking of chemical bonds, not involving a change in chemical groups. TRAP staining results are shown in Fig. 2F, G. The number and size of OCs were more than 50% inhibited by the addition of 10 μg/mL SFW-0.5-L and SFW-2-L treatment, and the inhibition effect of SFW-0.5-L is higher than 90% vs PBS. Meanwhile, at the level of gene transcription, 10 μg/mL SFW-0.5-L retained a repressive effect on the transcription of *Trap, Dc-Stamp, NFATc1*, and *ATP60*, achieving effects comparable to those of SFW-0.5 (Fig. 2D, H). In contrast, SFW-2-L showed a stronger ability to inhibit the expression of *Trap, Dc-Stamp, NFATc1*, and *ATP60* than SFW-2 but was still weaker than SFW-0.5-L (Fig. 2D, H). It has been hypothesized that changes in molecular weight affect the activity of SFs.

### Effect of desulfation on anti-OC differentiation of SFW-0.5, SFW-2

In order to investigate the effect of desulfation on the activity of SFW-0.5 and SFW-2, we chose to degrade them with HCl and then separated the degradation products by BioGel P-4 Gel (Fig. 2I, J). TRAP staining revealed that mature OCs were still formed after 10 μg/mL SFW-0.5-M and SFW-0.5-S treatment, while SFW-0.5-0 treatment effectively reduced the number and size of OCs to 20% vs PBS (Fig. 2K, L) after 5 days of RANKL induction. From the level of gene transcription, the ability of 10 μg/mL SFW-0.5-O to inhibit *Trap, Dc-Stamp, NFATc1*, and *ATP60* expression was the most prominent (Fig. 2M). Together with the above results, the SFW-0.5-O fraction was found to be an effective active component of SFW-0.5. Compared with the RANKL group, the treatment of SFW-2-M/S/O exerted an inhibitory effect on the differentiation and maturation of OC, and the size of OC was over half reduced; however, the number reduction was not significant (Fig. 2N, O). Neither SFW-2-M/S/O could effectively suppress the expression of related genes, and even SFW-2-S and SFW-2-O upregulated the expression of related genes (Fig. 2P). Therefore, we hypothesized that SF inhibited OC differentiation activity independent of the content of sulfate groups. Our results showed that SFW-0.5-O was the effective active component of SF and thus was selected for the follow-up study.

### Structure analysis of SFW-0.5-O

SFW-0.5-O polysaccharide was purified using a Bio-Gel P-10 column (2.6 × 100 cm), and six fractions were collected using 0.2 M ammonium bicarbonate as the mobile phase elution. The elution curves are shown in Fig. 3A. The results of the electrospray ionization (ESI)-MS analysis of the six samples showed that the components of A1 to A3 were too complex to be detected. Moreover, A4 showed that the major component was tetrasulfated galactofucan-pentamer (F4GS4, F stands for fucose, G stands for galactose, and S stands for sulfate). The figure stands for the number of the corresponding components. E.g., F4GS4 stands for four fucopyranose residues, one galactopyranose residue, and four sulfate groups. The major fraction of A5 was disulfated fucan-trimer (F3S2), and A6 was monosulfated-fucan-dimer (Fig. 3B–H).

Tandem ESI-MS with collision-induced dissociation (ESI-CID-$MS^2$) was performed to elucidate the structure. There were four major characteristic ions, i.e., $^{0,2}A_2$, $^{2,4}A_2$, $^{0,2}X_1$, and $^{0,3}X_1$. The presence of $^{0,2}A_2$ and $^{2,4}A_2$ suggested that the linkage of F2S is 1, 4-linked. Also, the presence of $^{0,2}X_1$ and $^{0,3}X_1$ suggested that the sulfation of F2S (Fig. 4A) is C2 sulfation at the non-reducing end. Accordingly, F2S was Fuc (2S)(1 → 4)Fuc. Figure 4B shows the ESI-CID-MS/MS spectrum of F3S2. F3S2 had similar characteristic ions to F2S, indicating they had similar components. The major difference was the ion at m/z 517.122, which was derived from the loss of sulfur trioxide with $H_2O$ (−98 Da), suggesting that the sulfation pattern might be C3 of fucopyranose residue. So F3S2 might be Fuc (2S)(1 → 4)Fuc(3S)(1 → 4)Fuc or Fuc (2S)(1 → 4)Fuc(1 → 4)Fuc(3S). The ESI-CID-$MS^2$ spectrum of the ion at m/z 270.022(-4), corresponding to F4GS4, had the strongest peak at m/z 279.024 (-3), which was derived from the loss of monosulfated fucopyranoside (FS) (Fig. 4C). Also, the ESI-CID-$MS^3$ spectrum of the ion at m/z 279.024 (-3), corresponding to F3GS3, showed two strong peaks at m/z 306.032 (-2) and 315.037 (-2), which were derived from the loss of dehydrated monosulfated fucopyranoside (FS) and FS (Fig. 4D). Also, the ESI-CID-$MS^4$ spectrum of the ion at m/z 315.037 (-2), corresponding to F2GS2, showed three intensive peaks at m/z 389.074 (-1), 405.068 (-1) and 533.115 (-1), which were derivated from the loss of dehydrated monosulfated galatopyranoside (GS), dehydrated FS and sulfur trioxide with $H_2O$, respectively (Fig. 4E). Therefore, it was concluded that F4GS4 might be FS-F-GS-FS-FS or FS-G-FS-FS-FS. The ESI-CID-$MS^2$ spectrum of F4GS5 (290.012(-4)) showed the strongest peak at m/z 270.022(-4), which was derivated from the loss of sulfur trioxide, indicating that F4GS5 might be FS-FS-GS-FS-FS or FS-GS-FS-FS-FS (Fig. 4F). In conclusion, SFW-0.5-O might have a backbone of alternating (Gal)n and (Fuc)n, and the major sulfation might be at C2/C3 of Fuc/Gal residues, as summarized in Fig. 4G.

### SFW-0.5-O inhibits OC differentiation

According to the cytotoxicity of SFs (Fig. S1), we chose the experimental doses of SFW-0.5-O for downstream experiments were 2.5, 5 and 10 μg/mL. TRAP staining demonstrated that treatment with SFW-0.5-O inhibited OC formation in a dose-dependent manner vs PBS (Fig. 5A, B) after 5 days of RANKL induction. In order to mediate efficient bone resorption, OCs must facilitate the efficient reorganization of the cytoskeleton to form a sealing zone[29]. We, therefore, evaluated the impact of SFW-0.5-O on actin ring formation in vitro. RANKL-treated cells exhibited a signature actin structural ring, consistent with a hallmark of OC maturation, and SFW-0.5-O treatment disrupted the formation of the actin ring in a dose-dependent trend (Fig. 5C) after 5 days of RANKL induction. These findings suggest that SFW-0.5-O inhibits OC maturation and cytoskeletal reorganization.

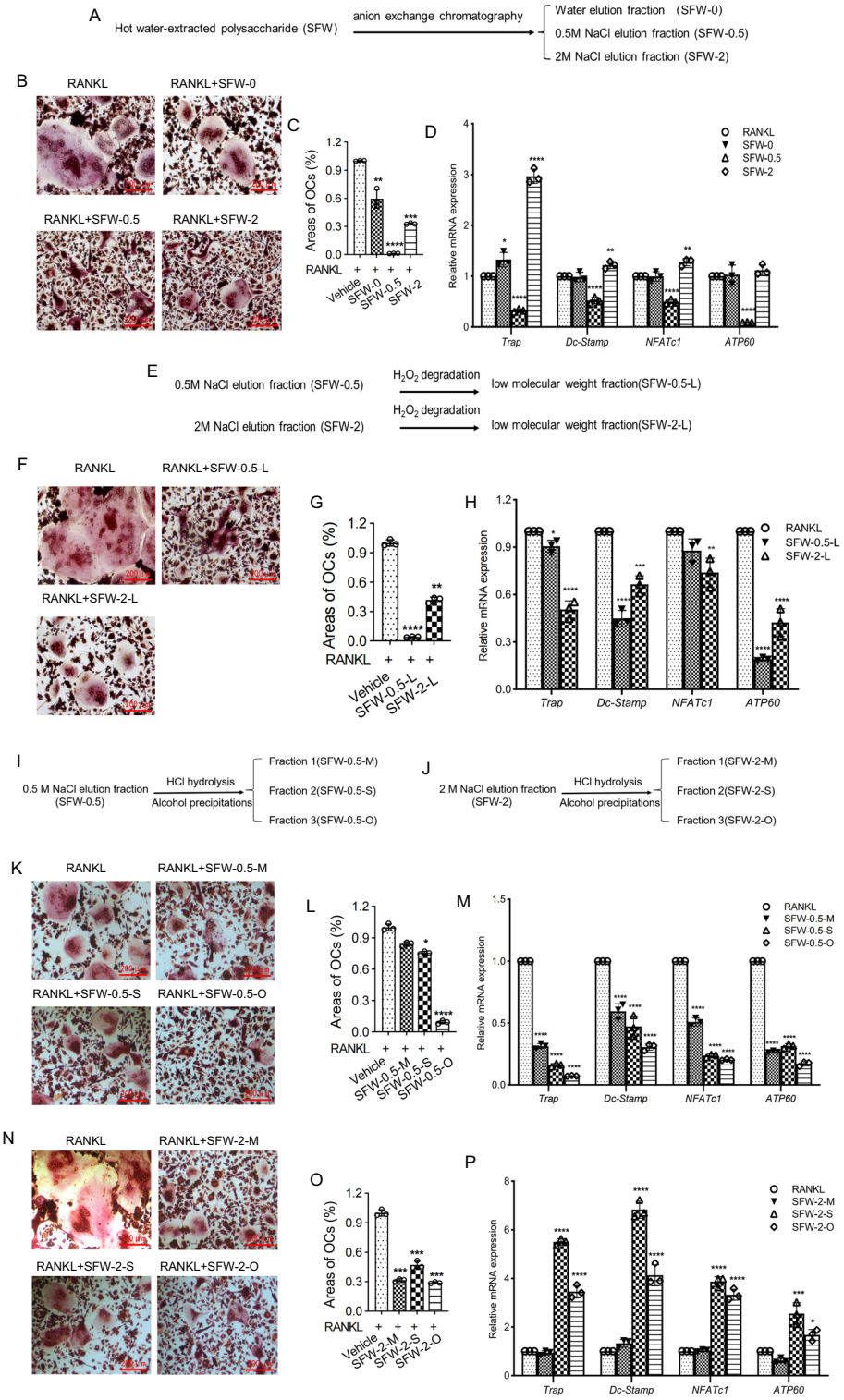


**Fig. 2 | Effect of molecular weight and desulfation of SF on inhibiting osteoclastogenesis. A** SFW was purified by anion exchange chromatography with elution by water, 0.5 M NaCl and 2 M NaCl to obtain different fractions (SFW-0, SFW-0.5 SFW-2). **B**, **C** TRAP staining of RAW264.7 was conducted following culture for 4 days with RANKL (50 ng/mL), and appropriate SFW-0, SFW-0.5, SFW-2, Scale bar = 200 μm. **D** RT- qPCR was used to assess the influence of SFW-0, SFW-0.5, SFW-2 on the expression of *Trap, DC-Stamp, NFATc1* and *ATP60*. **E** Hydrogen peroxide to oxidatively degrade the 0.5 M eluted fraction (SFW-0.5) and 2 M eluted fraction (SFW-2). **F**, **G** Suppression effect of SFW-0.5-L and SFW-2-L on osteoclastogenesis, Scale bar = 200 μm. **H** Influence of SFW-0.5-L and SFW-2-L on regulation of *Trap, DC-Stamp, NFATc1* and *ATP60*. **I**, **J** HCL hydrolysis of SFW-0.5 and SFW-2. **K**, **L** Suppression effect of SFW-0.5-M, SFW-0.5-S and SFW-0.5-O on osteoclastogenesis, Scale bar = 200 μm. **M** Influence of SFW-0.5-M, SFW-0.5-S and SFW-0.5-O on regulation of *Trap, DC-Stamp, NFATc1* and *ATP60*. **N**, **O** Suppression effect of SFW-2-M, SFW-2-S and SFW-2-O on osteoclastogenesis. **P** Influence of SFW-2-M, SFW-2-S and SFW-2-O on regulation of *Trap, DC-Stamp, NFATc1* and *ATP60*. Data are expressed as mean ± SD, n = 3. $^{*}P < 0.05$, $^{**}P < 0.01$ and $^{***}P < 0.001$ vs. RANKL.

We investigated the expression of genes related to the induction of OC differentiation by SFW-0.5-O on RANKL for 1 day (Fig. 5D, E) and 3 days (Fig. 5F, G) by qPCR. The expression of *Trap, Dc-Stamp, NFATc1*, and *ATP60*, which play important roles in OC differentiation, was significantly suppressed by SFW-0.5-O in a concentration-dependent manner on day 1 vs PBS (Fig. 5D), of which *NFATc1* declined by more than 90% at 10 μg/mL. IRF-8 as a critical negative regulator of OC differentiation was more than 80% suppressed by RANKL which was reversed by SFW-0.5-O treatment in a concentration-dependent manner on day 3 over five times, whereas Blimp1 is a negative regulator of IRF-8, SFW-0.5-O reduces its induced upregulation by RANKL (Fig. 5G).

We further examined the related protein expression changes after the induction of OC differentiation by appropriate SFW-0.5-O on RANKL for 24 h. The expression of NFATc1 and c-Fos was increased more than three times after RANKL stimulation, and SFW-0.5-O treatment decreased their expression levels even to base level in a concentration-dependent manner. In addition, as a suppressor of NFATc1, the expression of IRF-8 was decreased more than 50% by RANKL, and SFW-0.5-O upregulated its expression over 15% and showed a concentration-dependent manner.

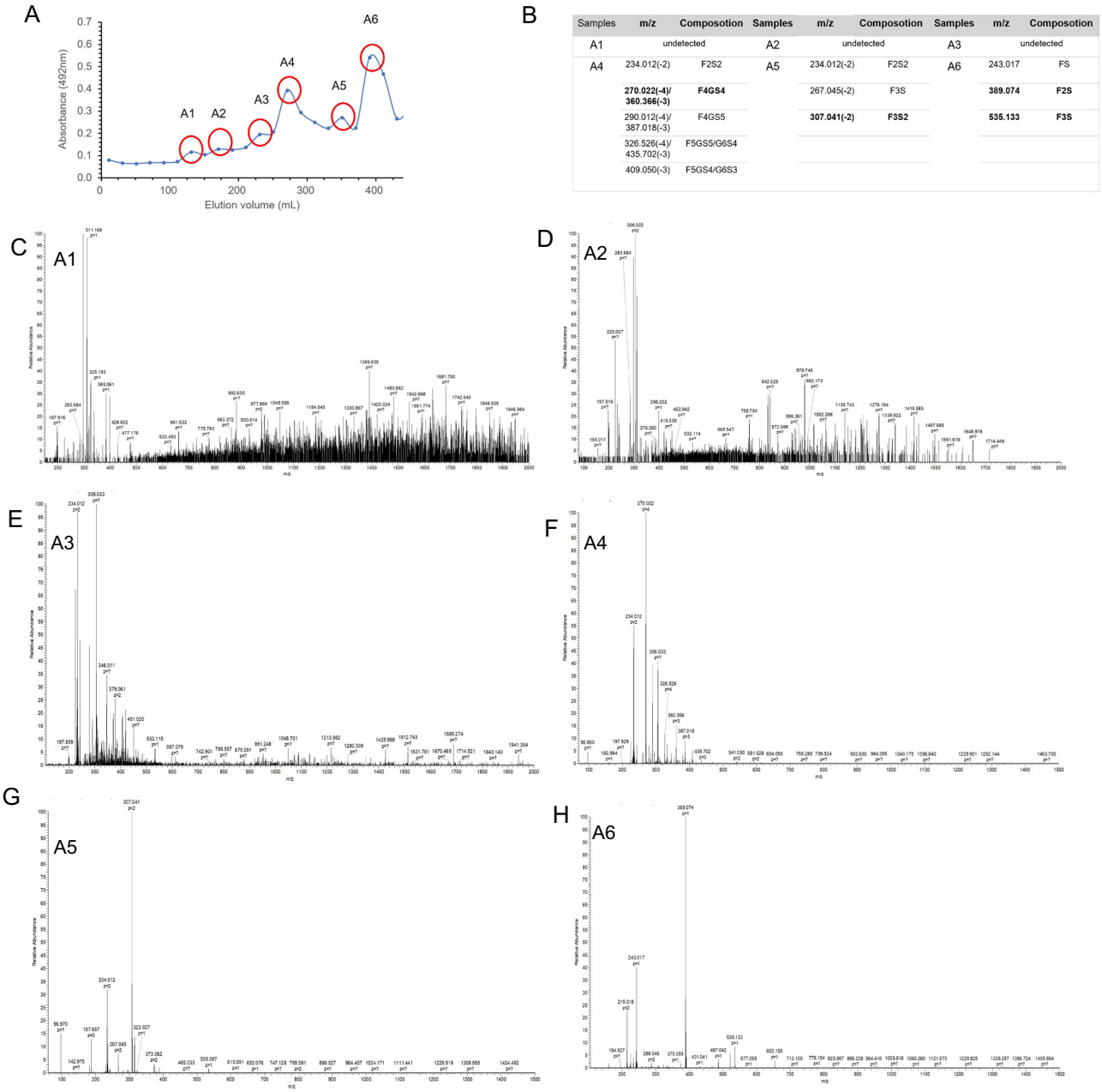


**Fig. 3 | The gel chromatography of SFW-0.5-O. A** Elution curves. **B** The primary compositions of A1 to A6, which were summarized in Table. **C–H** Negative-ion mode ESI-MS spectra of A1 to A6.

Blimp-1 negatively regulated the expression of IRF-8, and as we expected, SFW-0.5-O dose-dependently down-regulated the RANKL-induced increase in the expression of Blimp-1 more than 20%. SFW-0.5-O treatment attenuated the inhibitory effect of RANKL on IRF-8 expression, which was increased, thereby suppressing NFATc1 expression, and NFATC1 expression was reduced, resulting in a maximum over 50% reduction in Blimp-1 expression, which was alleviated and ultimately inhibited OC differentiation (Fig. 5H, I).

### SFW-0.5-O promotes OB differentiation

Next, we analyzed the effects of SFW-0.5-O on OB differentiation and mineralization. The proliferation results for MC3T3-E1 cells of SFW-0.5-O was shown in Fig. S1-B. ALP is a marker for early OB differentiation[30], whose activity was analyzed to reflect the early osteogenic potential of MC3T3-E1 cells. SFW-0.5-O respectively promoted ALP activity more than two times after treatment of SFW-0.5-O for 7 days (Fig. 5J) and enhanced the formation of the mineralized nodule (Fig. 5K, L) nearly four times as much at 10 μg/mL for 28 days in a concentration-dependent manner vs PBS. Our results also indicated that SFW-0.5-O promoted the expression of OB marker genes, such as *ALP* and *Runx2* (Fig. 5M). Osterix is an important transcription factor for OB differentiation and maturation, exerting its function by elevating the expression of ALP, Coll-1 etc[31]. SFW significantly elevated Osterix, ALP, and Coll-1 protein expression in a dose-dependent manner, of which ALP was boosted by more than double at 10 μg/mL. (Fig. 5N, O).

### SFW-0.5-O inhibits OVX-induced bone loss in vivo

The animal experiment workflow diagram is shown in Fig. 6A. OVX can induce fat accumulation and increase body weight[32]. SFW-0.5-O treatment reduced the weight gain caused by OVX around 2 g (Fig. 6B). Bone formation marker PINP and bone resorption marker β-CTx were

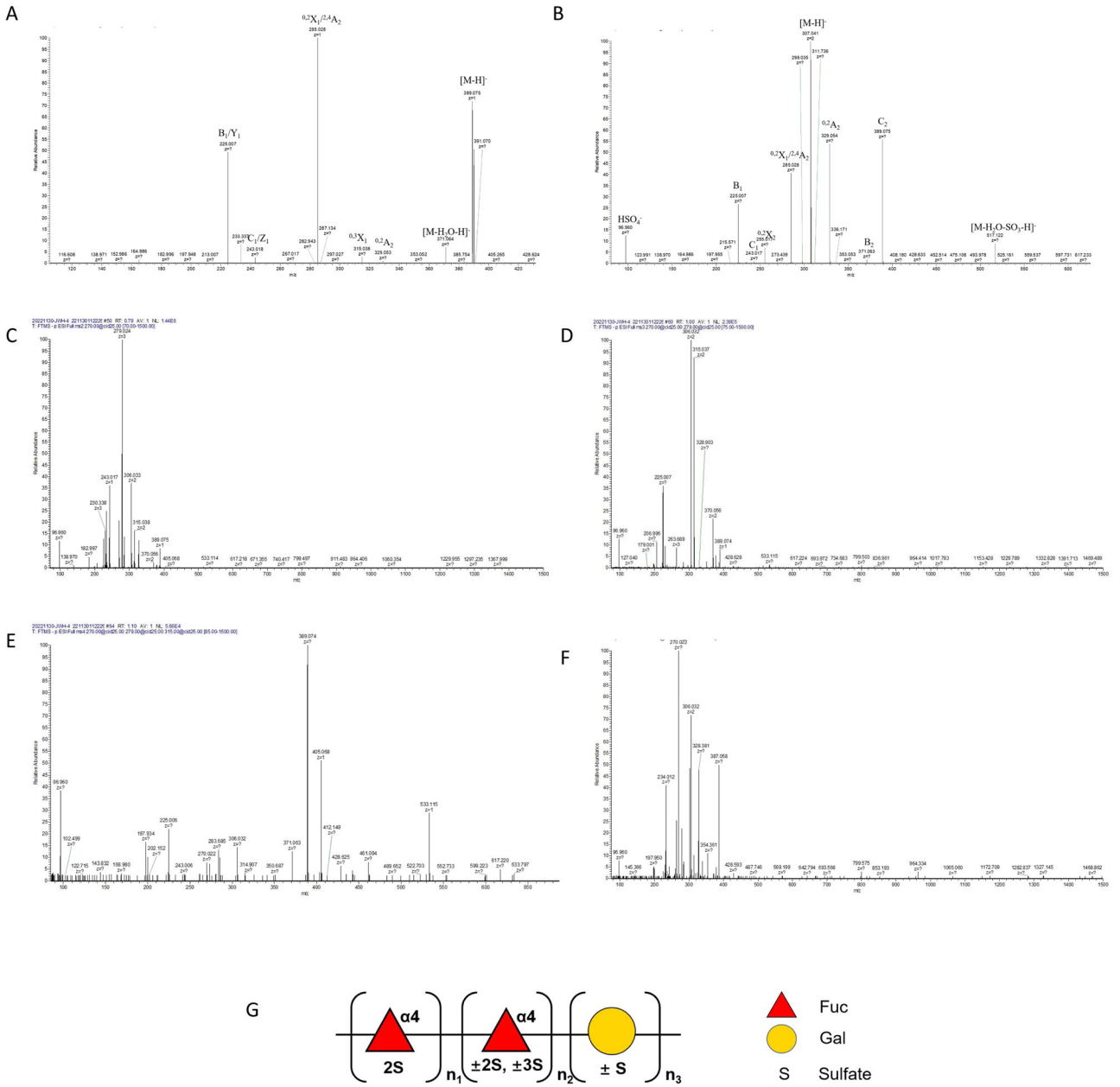


**Fig. 4 | Structure analysis of SFW-0.5-O. A** The negative-ion mode electrospray mass spectrometry in tandem with collision-induced dissociation tandem mass spectrometry (ESI-CID-$MS^2$) spectrum of the ion at m/z 389.074 (-1). **B** The ESI-CID-$MS^2$ spectrum of the ion at m/z 307.041(-2). **C** The ESI-CID-$MS^2$ spectrum of the ion at m/z 270.022 (-4). **D** The ESI-CID-$MS^3$ spectrum of the ion at m/z 279.024 (-3). **E** The ESI-CID-$MS^4$ spectrum of the ion at m/z 315.037 (-2). **F** The ESI-CID-$MS^2$ spectrum of the ion at m/z 290.012(-4). **G** Proposed structure of SFW-0.5-O.

measured by ELISA assay. As shown in Fig. 6C, D, serum PINP decreased more than 40% and serum β-CTx increased more than 35% in the OVX group mice. SFW-0.5-O treatment increased PINP concentration and decreased β-CTx concentration in a concentration-dependent manner, which showed that SFW-0.5-O treatment could effectively improve bone metabolism. SFW-0.5-O intervention did not significantly alter the metal ion concentration in the serum of OVX mice (Supplementary Fig. 2).

Representative microCT images with three-dimensional reconstruction of the cancellous and cortical bone of the femur are shown in Fig. 6E. MicroCT analyses of the femur samples from these animals confirmed that OVX treatment resulted in a lower bone mineral density (BMD) relative to sham control animals at 7 weeks post-ovariectomy. Treatment with a 10 mg/kg dose of SFW-0.5-O significantly improved BMD, inhibited trabecular bone loss as evidenced by an increasing ratio of bone volume to tissue volume (BV/TV), trabecular number (Tb.N) and reduced trabecular separation (Tb.Sp) in OVX animals. A higher SFW-0.5-O dose (20 mg/kg) was associated with even more significantly increased BMD, Tb.N, and trabecular thickness (Tb.Th), and decreased Tb.Sp (Fig. 6F–J).

We isolated BMMs from the femur of each group of mice and induced OC differentiation with RANKL. qPCR revealed that the transcript levels of the OC phenotype genes *Dc-Stamp, NFATc1*, and *ATP60* were higher in the OVX group of BMMs than in the Sham group and that estrogen deprivation increased the potential for OC differentiation. OC phenotype genes in the SFW-0.5-O intervention group of animals' transcript levels were significantly repressed, and the most pronounced repression was observed at high doses, showing a dose-dependent effect. As expected, the transcript levels of the OC differentiation regulatory gene *IRF-8* were elevated in the SFW-0.5-O

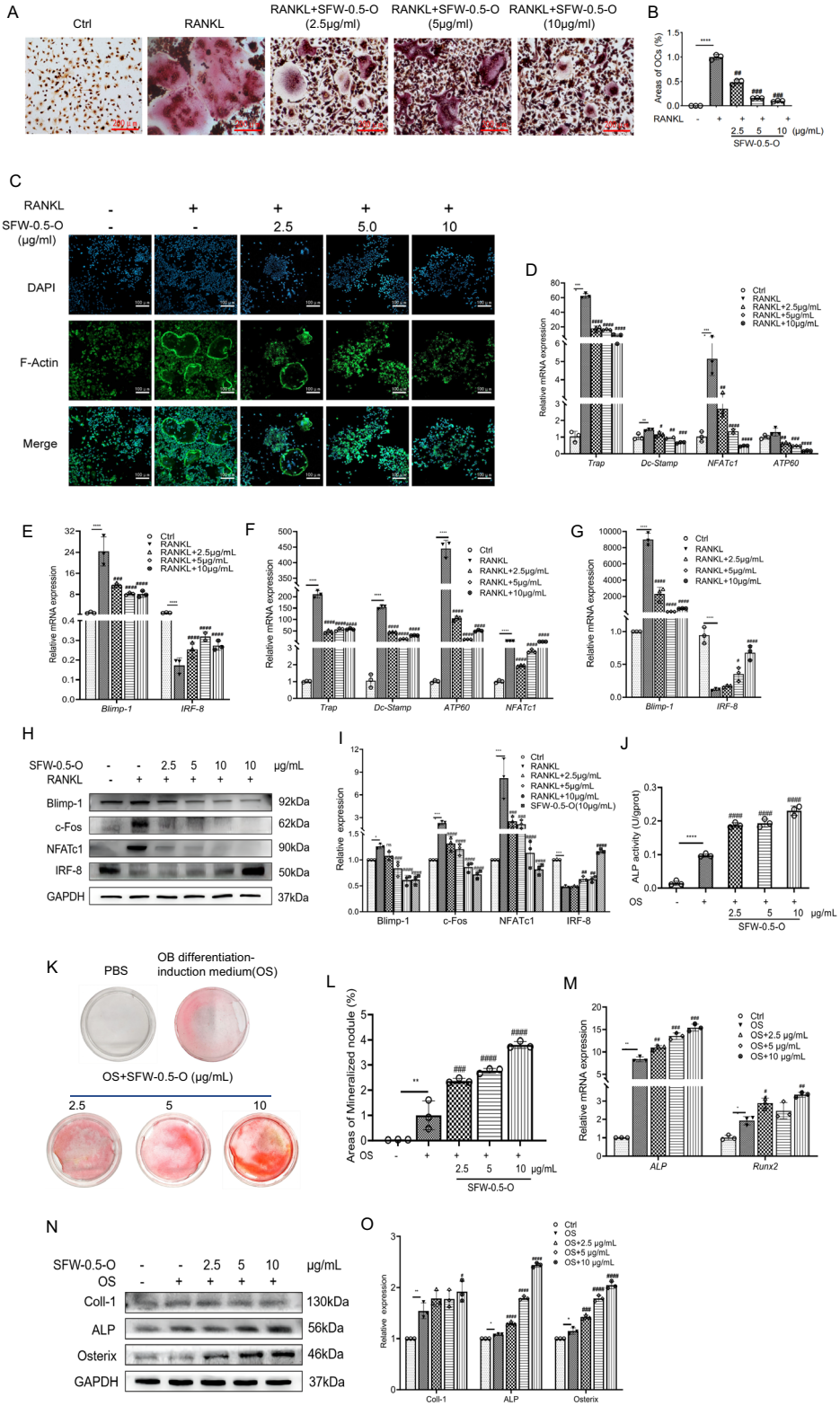


**Fig. 5 | SFW-0.5-O inhibits osteoclast differentiation and promotes osteogenic differentiation. A** TRAP staining of RAW264.7 was conducted following culture for 5 d with RANKL (50 ng/mL), and appropriate SFW-0.5-O concentrations (L: 2.5 μg/mL, M: 5 μg/mL, H: 10 μg/mL). **B** TRAP-positive cell area was quantified by Image J, Scale bar = 200 μm. **C** RAW264.7 cells were treated with RANKL and SFW-0.5-O for 5 d, and the representations images were stained by F-actin staining. Scale bar = 100 μm. RT-qPCR for OC-related genes after treatment of RANKL and appropriate SFW-0.5-O for 1 d (**D**, **E**) and 3 d (**F**, **G**). **H**, **I** WB for OC differentiation regulatory proteins after treatment of RANKL and appropriate SFW-0.5-O for 24 h. **J** ALP activity after 7 d of osteogenesis differentiation induction. **K** Alizarin red staining for bone mineral nodules. **L** Percentage of bone mineral nodules area. **M** RT- qPCR for OB-related genes after treatment of appropriate SFW-0.5-O. **N**, **O** WB for OB differentiation regulatory proteins after treatment of appropriate SFW-0.5-O. All semi-quantitative analyses were conducted by Image J. Data are expressed as mean ± SD, n = 3. $^{*}$ $P < 0.05$, $^{**}$ $P < 0.01$ and $^{***}$ $P < 0.001$*vs.* CTRL; $^{\#}$ $P < 0.05$, $^{\#\#}$ $P < 0.01$ and $^{\#\#\#}$ $P < 0.001$ vs. RANKL or OS.

intervention compared to the OVX group, and the highest transcript levels were found in the high-dose group, with a relative decrease in Blimp-1 transcript levels (Fig. 6K, L).

We examined the expression levels of osteoclastic differentiation-related proteins after induced differentiation of primary BMMs. As shown in Fig. 6M, N, the expression levels of NFATc1 and Blimp-1 were increased more than three times in the OVX group. Also, c-fos showed an increasing trend, while IRF-8 expression was decreased over half. However, the corresponding trend was reversed in the SFW-0.5-O treated group, where the high dose of SFW-0.5-O increased the level of IRF-8 up to 90% of the base level.

In conclusion, our results suggest that SFW-0.5-O inhibits OC differentiation at least in part by increasing IRF-8 levels in OVX mice, which could be used to explain its role in enhancing the reduction in bone mass and improving microarchitectural bone degeneration caused by estrogen deprivation.

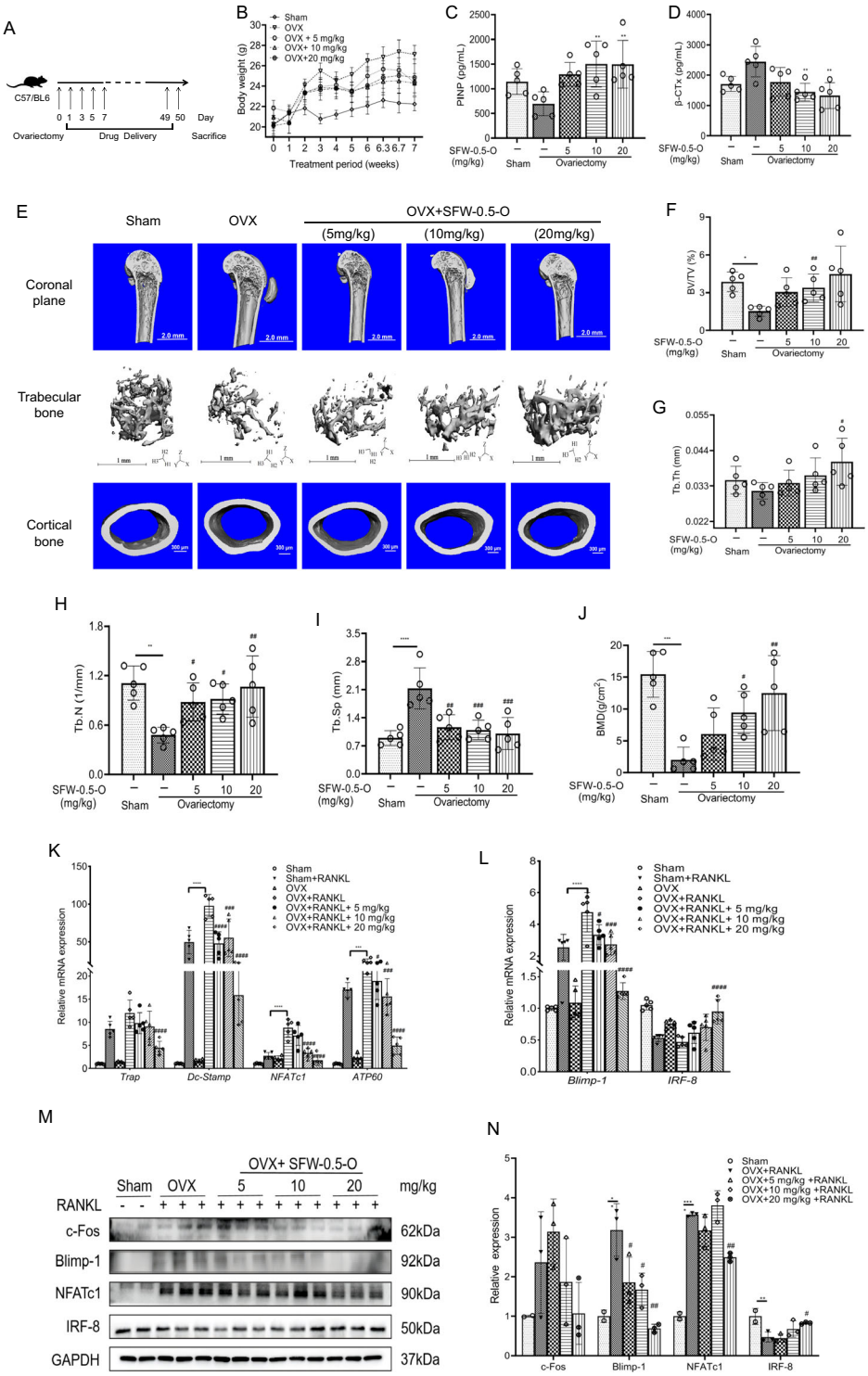


**Fig. 6 | SFW-0.5-O protects against bone loss.** **A** Animal experiment workflow. **B** Body weight of mice in each group. **C**, **D** Serum levels of PINP and β-CTx. **E** Representative images with three-dimensional reconstruction of the mouse femur. Trabecular bone parameters including (**F**) Volume of bone to tissue (BV/TV), (**G**) trabecular thickness (Tb. Th), (**H**) trabecular bone number (Tb. N), and (**I**) trabecular separation (Tb. Sp) of each sample were calculated and analyzed (n = 5). **J** Bone marrow density (BMD) at femurs was detected by X-ray absorptiometry (n = 5). **K**, **L** RT-qPCR for OC-related genes. **M**, **N** WB for OC differentiation regulatory proteins in induced BMMs cells. Data are expressed as mean ± SD, n = 3. $^{*}P < 0.05$, $^{**}P < 0.01$ and $^{***}P < 0.001$ *vs*. Sham; $^{\#}P < 0.05$, $^{\#\#}P < 0.01$ and $^{\#\#\#}P < 0.001$ vs. OVX.

## Discussion

OP is one of the most commonly encountered degenerative bone diseases in an aging society, leading to bone fragility and increased risk of fractures. Current studies in this field have been focusing on searching for potential and safer natural substances that could be obtained from food to replace existing drugs to treat OP, thus eliminating the side effects of drug therapy. SF has been proven to regulate bone remodeling by inhibiting OC differentiation[33] or promoting OB formation[19], thus exerting osteoprotective effects[34] effects. A byproduct of *Hizikia fusiforme* (HFB) has also been shown to have osteoprotective effects. While previous studies have focused more on crude SF, the overall structure of SF and the specific active ingredients still remain unclear[35]. On the basis of our predecessor, we carried out studies to further explore the unidentified active component of SF for improving OP symptoms by structure-activity relationship analysis, which suggested that it might be a valuable compound.

Different extraction methods can produce significant differences in bioactive substances' molecular structure and composition. Generally, standard SF extraction methods can be divided into three categories: dilute acid, alkali, and hot water extraction methods[36]. The SF is a mixture and requires rigorous purification by fractional precipitation, ion exchange column chromatography, membrane filtration, size exclusion chromatography, or affinity chromatography. The method of extraction is decisive for

the molecular size of the SF since high temperatures induce molecular breakage, leading to fragmentation, and the use of strong chemicals introduces chemical groups into the structure[37]. Accordingly, we investigated the extraction method's effect on SF's OC suppression capacity. We found that the SF extracted by hot water had better OC differentiation inhibitory activity than acid and alkaline extraction methods (Fig. 1). The SFW was passed through an anion-exchange column and eluted with 0, 0.5, and 2 M NaCl to obtain SFW-0/0.5/2. Our results showed that the SFW-0.5 fraction had the strongest biological activity to inhibit OC differentiation (Fig. 2), which is related to their different carbohydrate content and sulfation degree components. The unique chemical structure and composition of fuciodan confers a variety of biological activities, such as molecular size, sulfate content, and even the distribution of sulfate groups that affect its biological activity [37–39]. We investigated the effect of molecular weight on the ability of SFs to inhibit OC differentiation and degraded SFW-0.5 and SFW-2 by $H_2O_2$ oxidation to obtain the low molecular weight fractions SFW-X-L. Our results showed that both SFW-0.5-L and SFW-2-L effectively inhibited OC differentiation, as evidenced by the morphology of OC and the transcription of genes associated with OC differentiation. The inhibitory effect of SFW-2-L on OC differentiation was significantly stronger than that of SFW-2, indicating that the lower molecular weight SFs had a stronger ability to inhibit OC differentiation (Fig. 2B–H).

Previous studies have focused on investigating whether sulfate groups' content affects SF's biological activity. It has been reported that the degree of sulfation of SF affects its antioxidant activity and anticoagulant activity [37]. However, it has also been found that the anti-HIV activity of SF is independent of the sulfate group content and the position of the sulfate group in the backbone[40]. Therefore, we investigated the effect of sulfate group content on the ability of SF to inhibit OC differentiation. SFW-2 and the three fractions obtained after desulfurization (SFW-2-M/S/O) did not significantly inhibit OC differentiation (Fig. 2D, N–P) compared to SFW-0.5, which had stronger inhibitory activity on OC itself. In addition, the three fractions obtained after desulfurization (SFW-0.5-M/S/O) could significantly inhibit OC differentiation, among which SFW-0.5-O had the best inhibitory activity on OC (Fig. 2D, K–M). Therefore, we concluded that desulfurization did not affect the biological activity of SFs in inhibiting OC differentiation. Together with the above structure-activity relationship analysis, we confirmed that SFW-0.5-O is the anti-OC active ingredient of SF extracted from *Sargassum fusiforme*.

Immediately after, we analyzed the structure of the SFW-0.5-O. First, we purified the SFW-0.5-O polysaccharide by a Bio-Gel P-10 column and eluted it with 0.2 M ammonium bicarbonate as the mobile phase to obtain six fractions. Then, electrospray ionization (ESI)-MS analysis revealed that the composition of A1, A2 and A3 was too complex to be detected. The main component of A4 was a tetrasulfated galactose pentamer (F4GS4, F for fucose, G for galactose, S for sulfate), the main component of A5 was a disulfated rockweed trimer (F3S2), and A6 was a monosulfated rockweed dimer (Fig. 3). Tandem ESI-MS with collision-induced dissociation (ESI-CID-MS2) was used to elucidate the structure. Finally, we speculated that SFW-0.5-O might have an alternating backbone of (Gal)n and (Fuc)n, and the main sulfation might be at C2/C3 of Fuc/Gal residues. The structure resolution process and structural schematic are shown in Fig. 4.

OC and OB model systems and ovariectomized animal models were used to demonstrate the utility and mechanism of SFW-0.5-O against OP in vitro and in vivo as an alternative therapy for OP. In regulating OC differentiation, SFW-0.5-O effectively inhibited OC differentiation and down-regulated RANKL-induced enhanced transcription of OC phenotype genes as observed by morphological staining and cytoskeletal remodeling. All of the above effects were found to be dose-dependent (Fig. 5A–G). IRF-8 is an essential regulatory protein for OB differentiation. Our previous study confirmed that IRF-8 is one of the targets of oligosaccharides from *Sargassum thunbergii* to inhibit OC differentiation[16]. Our assay revealed that SFW-0.5-O dose-dependently and significantly elevated RANKL-induced IRF-8 downregulation while downregulating the expression of OC differentiation transcriptional regulators c-fos and NFATc1 (Fig. 5H, I). Strikingly, SFW-0.5-O also showed significant promotion of osteogenic differentiation, as evidenced by its promotion of osteomineralized nodule production, transcription of the osteogenic differentiation regulatory genes ALP and Runx2, and upregulation of the expression of the osteogenic differentiation regulatory proteins ALP, Coll-1 and Osterix in a dose-dependent manner (Fig. 5K–O). As expected, the in vivo study confirmed that SFW-0.5-O effectively ameliorated bone loss caused by estrogen deprivation, which was demonstrated by reversing the decrease in the bone formation marker PINP and the increase in the bone resorption marker β-CTx caused by ovariectomy. Improved degeneration of bone trabecular microarchitecture while increasing bone mass was observed, as shown in (Fig. 6A–J). Primary isolated BMMs induced by RANKL revealed that SFW-0.5-O effectively repressed the potential transcriptional capacity of OC differentiated genes in vivo and exhibited significant regulation of IRF-8 signaling at both the transcriptional and protein levels. Also, the regulation was more pronounced at high concentrations (Fig. 6K–N).

In summary, we have confirmed for the first time that sulfated galactofucan (SFW-0.5-O) is an osteoprotective ingredient of SFs of *Sargassum fusiforme* origin through a meticulous structure-activity relationship analysis. These findings provide new evidence that SFW-0.5-O may have potential value in treating OP. In terms of mechanism of action, we determined that SFW-0.5-O inhibits OC differentiation and bone resorption at least partially through the upregulation of IRF-8; however, the precise mechanism of its osteoprotective effects should be further investigated by future studies.

## Materials and methods

### SF and its hydrolysis fractions preparation

The brown seaweed *Sargassum fusiforme* was collected in Zhanjiang Province, China. Polysaccharides (SFS, SFJ, SFW) were extracted by acid extraction (0.1 M HCl), alkali extraction (5% $Na_2CO_3$), and hot water extraction according to the reported preparation methods in our laboratory[41]. SFW was purified by anion exchange chromatography on a DEAE-Bio Gel Agarose FF gel (6 cm × 40 cm) with elution by water (SFW-0), 0.5 M NaCl (SFW-0.5) and 2 M NaCl (SFW-2) at a flow rate of 10.0 mL/min to obtain different fractions. Next, SFW-0.5 and SFW-2 were degraded by oxidation with $H_2O_2$ to obtain SFW-0.5-L and SFW-2-L, respectively. Next, SFW-0.5 and SFW-2 were subjected to HCl degradation and two alcohol precipitations to obtain SFW-0.5-M, SFW-0.5-S, SFW-0.5-O, and SFW-2-M, SFW-0.5-S, SFW-0.5-O with different molecular weights, respectively. Structural analysis by Electrospray Ionization Mass Spectrometry (ESI-MS)/Electrospray Ionization Mass Spectrometry - Collision Induced Dissociation - Multi-stage Mass Spectrometry(ESI-CID-MSn), which were widely used techniques for molecular weight identification of polysaccharides, was used to analyze the structure of the SFW-0.5-O.

### Cell culture

The tenth passage of RAW264.7 cells and MC3T3-E1 cells (ATCC, Manassas, USA) were cultured in minimum essential medium α (MEM α; Gibco, USA) with 10% fetal bovine serum (Gibco, USA) and 100 U/mL streptomycin/penicillin (Gibco, USA) in a humidified atmosphere containing 5% $CO_2$/95% air at 37 °C.

### Cell proliferation assays

Cultured cells were plated in 96-well plates ($4 \times 10^3$ cells/well) with α-MEM medium which contained approximately 20, 40, 60, 80 μg/mL concentrations of SFs for RAW264.7 and 2.5, 5, 10, 20, 30 μg/mL concentrations of SFW-0.5-O for MC3T3-E1. PBS was used as vehicle. 48 h later, 10 μL 5.0 mg/mL methyl thiazolyl diphenyl-tetrazolium bromide (MTT; Sigma-Aldrich, USA) was added to each well. Following incubation for 4 h at 37 °C, the supernatant was removed, and 150 μL DMSO was added. Subsequently, absorbance was measured by optical density (OD) at 490 nm, and the cell viability results with blank group without SF as 100%.

### In vitro assessment of osteoclastogenesis

TRAP staining was performed to assess osteoclastogenesis. RAW264.7 cells ($1 \times 10^3$ cells/well) were plated into 24-well plates with appropriate SFs concentrations (10 μg/mL or 2.5, 5, and 10 μg/mL) and 50 ng/mL RANKL (R&D Systems, USA) for 5 days, while the medium was changed every two days, after which cells were washed with PBS, fixed with 4% paraformaldehyde (PFA), and stained with a TRAP staining kit (Sigma-Aldrich, MO, USA)[42]. TRAP-positive cell area was quantified by Image J.

Immunofluorescence assay was used to assess F-actin ring formation. As for the experiment of F-actin ring formation, RAW264.7 cells were seeded in dedicated culture dishes for 24 h. After initial incubation, 50 ng/mL RANKL and appropriate concentrations of SF (2.5, 5, 10 μg/mL) were added to triplicate wells, and the medium was changed every two days for 5 days. PBS was used as vehicle. Next, cells were rinsed with PBS, fixed with 4% Paraformaldehyde (Sigma-Aldrich, USA) for 30 min, blocked with 5% BSA after washing with PBS, and then stained with F-actin (Abcam, UK) and DAPI (Sigma-Aldrich, USA). Cells were then evaluated by confocal immunofluorescence (ZEISS, NY, USA)[43].

### Alizarin red S staining

MC3T3-E1 cells ($1 \times 10^5$ cells/dish) were grown in an OB differentiation-induction medium (OS) in 35 mm dishes, which was supplemented with 10 mM beta-glycerophosphate, 100 μg/mL ascorbic acid, and $10^{-8}$ M dexamethasone with appropriate SFs concentrations (2.5, 5, and 10 μg/mL). PBS was used as vehicle. Alizarin Red S staining determined calcium deposition in the extracellular matrix after 28 days of osteogenic differentiation. Cells were fixed in 4% Paraformaldehyde and then incubated in 0.1% Alizarin Red S solution (pH = 4.3; Sigma-Aldrich, USA). Calcium deposition was observed and visualized under a light microscope[44]. Areas of mineralized nodule were quantified by Image J.

### qPCR and Western blot

After 1 and 3 days of RANKL induction, RAW264.7 cells were harvested for RNA extraction with an RNA extraction kit (Yishan Bio., China). Moreover, MC3T3-E1 cells were treated with OB differentiation-induction medium for 7 days. The SF intervention groups were simultaneously administered 2.5, 5, and 10 μg/mL of SFs. PBS was used as vehicle. Genes expression levels were detected by qPCR using the SYBR Green Realtime PCR Master Mix -Plus (Vazyme, China). The total cDNA abundance between samples was normalized using the glyceraldehyde-3-phosphate dehydrogenase (GAPDH) gene, with the $2^{-\Delta\Delta Ct}$ approach being used to assess relative gene expression. The primers[11,16,45,46] used in this protocol are presented in Table 1.

For Western blot, RAW264.7 cells were plated in 6-well plates ($1 \times 10^5$ cells/ well). After incubating for 12 h, RAW264.7 cells were treated with RANKL in the absence and presence of SFs for 24 h. Moreover, MC3T3-E1 cells were plated into 6-well plates with different concentrations of SF and OB differentiation-induction medium in a 5% $CO_2$ humidified incubator at 37 °C for 7 days, and the medium was changed every 2 days. Western blotting was performed as previously described[47]. The following primary antibodies were used: IRF-8, Blimp-1, NFATc1, and c-Fos antibodies (Cell Signaling Technology, USA); Coll-1, ALP, Osterix (Abcam, UK); GAPDH antibody (Santa Cruz, USA).

### Alkaline phosphatase (ALP) assay

Conventional osteogenic induction medium was used for ALP assay. The formulation of the induction medium was as above. MC3T3-E1 cells were inoculated in 24-well plates ($2 \times 10^4$ cells/well) and cultured for 24 h. After 24 h of incubation, SFW-0.5-O was added to the osteogenic induction medium in a concentration gradient of 2.5, 5, and 10 μg/mL. Fresh osteogenic induction differentiation medium containing SFW-0.5-O was replaced every 3 days. PBS was used as vehicle. Cells were collected for analysis after 7 days. Alkaline phosphatase activity and protein content of the cells were determined using the Alkaline Phosphatase Assay Kit (Jiancheng Bioengineering, China) and BCA Protein Assay Kit. ALP activity was calculated based on protein content.

### Ovariectomized mouse model

The OVX mouse model is well-established for PMOP[48], The 8-week-old female C57BL/6J mice were housed in a temperature and humidity-controlled barrier facility with free access to water and food and a 12-h light/dark cycle. After 1 week of habituation to the environment, mice were randomly divided into 5 following groups: sham-operated group (Sham), OVX group, and OVX group treated with low/medium/high SFW-0.5-O concentrations (OVX-L/M/H). Mice in the OVX and OVX-L/M/H groups underwent bilateral ovariectomy, while in mice in the Sham group, the skin was only opened to find the ovaries and was sutured without ovariectomy. Referring to our previously published results that SFs had low in vivo toxicity and superior biological activity[49,50], we first selected lower concentrations for in vivo studies. Immediately after grouping, the fucoidan intervention group were administered L/M/H concentrations of SFW-0.5-O (5, 10, or 20 mg/kg) by intraperitoneal injection for 50 consecutive days at one day intervals. Mice in the sham-operated and model groups were injected with equal volumes of saline.

All mice were housed in specific pathogen-free facility, and animal procedures performed in this study were consistent with the National Research Council's Guide for the Care and Use of Laboratory Animals (NIH, USA) and were approved by the Animal Care Committee of Zhejiang University (IACUC, ZJU20200149) in accordance with the National Research Council's Guide for the care and Use of Laboratory Animals.

### Micro-computed tomography scanning

The femur from euthanized animals were fixed in 4% paraformaldehyde for 48 h, after which it was washed with phosphate-buffered saline (PBS), and transferred into 70% ethylalcohol for micro-computed tomography (μCT) scanning and three-dimensional reconstruction (μCT40; Scanco Medial, Switzerland). The morphological characteristics of the femoral trabeculae and cortical bone were studied to analyze the skeletal changes. The trabecular

**Table 1 | Primer sequences for the indicated genes**

| Gene | Forward (5' to 3') | Reverse (5' to 3') |
|---|---|---|
| DC-Stamp | ACAAACAGTTCCAAAGCTTGC | TCCTTGGGTTCCTTGCTTC |
| NFATc1 | CCGTTGCTTCCAGAAAATAACA | TGTGGGATGTGAACTCGGAA |
| ATP60 | AAGCCTTTGTTTGACGCTGT | TTCGATGCCTCTGTGAGATG |
| IRF-8 | GGGCTGATCTGGGAAAATGA | CACCTCCTGATTGTAATCC- TGCTT |
| Trap | CTGGAGTGCACGATGCCAGCGACA | TCCGTGCTCGGCGATGGACCAGA |
| Blimp-1 | TTCTTGTGTGGTATTGTCGGGACTT | TTGGGGACACTCTTTGGGTAGAGTT |
| ALP | ATCTTTGGTCTGGCTCCCATG | TTTCCCGTTCACCGTCCAC |
| Runx2 | TTTGCAGTGGGACCGACA | AGCCATGGTGCCCGTTAG |
| GAPDH | ACCCAGAAGACTGTGGATGG | CACATTGGGGGTAGGAACAC |

bone in the tibia was quantified with 100 μCT slices (1.6 mm) immediately below the growth plate. The volume of bone to tissue (%), trabecular thickness (mm), trabecular bone number (1/mm), and trabecular separation (mm) were determined to investigate the trabecular structure.

### Isolation of bone marrow-derived monocytes (BMMs)

BMMs were cultured in α-MEM medium containing 40 ng/mL of M-CSF for 48 h to adhere to the plate, after which the unadhered cells were discarded, and α-MEM containing M-CSF was added until the cells fused. Moreover, 50 ng/mL RANKL was treated for 1 d for qPCR experiments and for 3 d for Western blot experiments to assess the effect of appropriate SFW-0.5-O concentrations on osteoclastogenesis using above described operation methods.

### Serum markers of bone metabolism

Blood was collected and left overnight at 4 °C. After centrifugation at 3000 rpm for 5 min, serum was collected, and an enzyme-linked immunosorbent kit (Elabscience, China) was used to detect serum type I procollagen N-terminal peptide (PINP) and β-collagen crosslinking (β-CTx) in each group. Serum metal ion concentration was measured with a fully automated biochemical analyzer (Beckman AU5400, USA).

### Statistics and reproducibility

Data are presented as mean ± SD. In vitro experiments were repeated three times; for in vivo studies, five mice were set up in each group. All statistical tests were performed using SigmaStat 2.0 (SPSS Inc., IL, USA). All data were normally distributed. Data were analyzed using One-way ANOVAs and the Student's *t* test. $P < 0.05$ and $P < 0.01$ were the significance thresholds in this study. All experiments were repeated in triplicate, and representative results are shown.

### Statistics and reproducibility

Statistical tests employed and significance cut-off values are indicated per experiment in the "Methods" section. The statistical analyses conducted on the data in each figure were described in their respective figure captions. Experiments were performed with three independent repeats.

### Reporting summary

Further information on research design is available in the Nature Portfolio Reporting Summary linked to this article.

## Data availability

Source Data for Figs. 1–6 and Supplementary Figs. 1 and 2 are available in Supplementary Data 1. Uncropped images of blots/gels are available in Supplementary Figs. All other relevant data are available from the corresponding author on reasonable request.

## Abbreviations

| | |
|---|---|
| SF | fucoidan |
| SFS | Fucoidan from Sargassum fusiforme Extracted from Acid |
| SFJ | Fucoidan from Sargassum fusiforme Extracted from Alkaline |
| SFW | Fucoidan from Sargassum fusiforme Extracted from Water |
| OC | osteoclast |
| OB | osteoblast |
| SAR | structure-activity relationship |
| SFW-x-L | SF with low molecular weight (x for 0.5 or 2); SFW-x-M/S/O: dilute acid degradation products of SFW-x (x for 0.5 or 2) |

Received: 18 April 2024; Accepted: 17 October 2024;
Published online: 08 November 2024

## References

1. Imam, B., Aziz, K., Khan, M., Zubair, T. & Iqbal, A. Role of bisphosphonates in postmenopausal women with osteoporosis to prevent future fractures: a literature review. *Cureus* **11**, e5328 (2019).
2. Feng, X. & McDonald, J. M. Disorders of bone remodeling. *Annu. Rev. Pathol.* **6**, 121–145 (2011).
3. Li, J., Chen, X., Lu, L. & Yu, X. The relationship between bone marrow adipose tissue and bone metabolism in postmenopausal osteoporosis. *Cytokine Growth Factor Rev.* **52**, 88–98 (2020).
4. Deeks, E. D. Denosumab: a review in postmenopausal osteoporosis. *Drugs Aging* **35**, 163–173 (2018).
5. Gregson, C. L. et al. UK clinical guideline for the prevention and treatment of osteoporosis. *Arch Osteoporos* **17**, 58 (2022).
6. Black, D. M. et al. Atypical femur fracture risk versus fragility fracture prevention with bisphosphonates. *N. Engl. J. Med.* **383**, 743–753 (2020).
7. Wei, H. et al. Identification of fibroblast activation protein as an osteogenic suppressor and anti-osteoporosis drug target. *Cell Rep.* **33**, 108252 (2020).
8. Lyritis, G. P., Georgoulas, T. & Zafeiris, C. P. Bone anabolic versus bone anticatabolic treatment of postmenopausal osteoporosis. *Ann. N Y Acad. Sci.* **1205**, 277–283 (2010).
9. Garnero, P., Sornay-Rendu, E., Chapuy, M. C. & Delmas, P. D. Increased bone turnover in late postmenopausal women is a major determinant of osteoporosis. *J. Bone Miner. Res.* **11**, 337–349 (1996).
10. Xiao, F. et al. Geraniin suppresses RANKL-induced osteoclastogenesis in vitro and ameliorates wear particle-induced osteolysis in mouse model. *Exp. Cell Res.* **330**, 91–101 (2015).
11. Xia, X., Wang, W., Yin, K. & Wang, S. Interferon regulatory factor 8 governs myeloid cell development. *Cytokine Growth Factor Rev.* **55**, 48–57 (2020).
12. Jacome-Galarza, C. E. et al. Developmental origin, functional maintenance and genetic rescue of osteoclasts. *Nature* **568**, 541–545 (2019).
13. Zhao, B. et al. Interferon regulatory factor-8 regulates bone metabolism by suppressing osteoclastogenesis. *Nat. Med.* **15**, 1066–1071 (2009).
14. Izawa, N. et al. Cooperation of PU.1 With IRF8 and NFATc1 defines chromatin landscapes during RANKL-Induced Osteoclastogenesis. *J. Bone Miner. Res.* **34**, 1143–1154 (2019).
15. Saito, E. et al. Down-regulation of Irf8 by Lyz2-cre/loxP accelerates osteoclast differentiation in vitro. *Cytotechnology* **69**, 443–450 (2017).
16. Jin, W., Chen, F., Fang, Q., Mao, G. & Bao, Y. Oligosaccharides from Sargassum thunbergii inhibit osteoclast differentiation via regulation of IRF-8 signaling. *Exp. Gerontol.* **172**, 112057 (2023).
17. Schlesinger, P. H. et al. Cellular and extracellular matrix of bone, with principles of synthesis and dependency of mineral deposition on cell membrane transport. *Am. J. Physiol. Cell Physiol.* **318**, C111–C124 (2020).
18. Shim, N. Y., Ryu, J. I. & Heo, J. S. Osteoinductive function of fucoidan on periodontal ligament stem cells: role of PI3K/Akt and Wnt/beta-catenin signaling pathways. *Oral Dis.* **28**, 1628–1639 (2022).
19. Kim, B. S., Kang, H. J., Park, J. Y. & Lee, J. Fucoidan promotes osteoblast differentiation via JNK- and ERK-dependent BMP2-Smad 1/5/8 signaling in human mesenchymal stem cells. *Exp. Mol. Med.* **47**, e128 (2015).
20. Jeong, H. S., Venkatesan, J. & Kim, S. K. Hydroxyapatite-fucoidan nanocomposites for bone tissue engineering. *Int. J. Biol. Macromol.* **57**, 138–141 (2013).
21. Deng, L. et al. Isolation and characterization of a novel homopolysaccharide (SFP-1) from Sargassum fusiforme: Promising anti-osteoporosis activity by modulating adipo-osteogenic differentiation. *Ind. Crops Products* **207**, https://doi.org/10.1016/j.indcrop.2023.117749 (2024).

22. Gupta, D., Martinez, D. C., Puertas-Mejia, M. A., Hearnden, V. L. & Reilly, G. C. The effects of Fucoidan Derived from *Sargassum filipendula* and Fucus vesiculosus on the Survival and Mineralisation of Osteogenic Progenitors. *Int. J. Mol. Sci.* **25**, https://doi.org/10.3390/ijms25042085 (2024).
23. Lu, S. H., Hsia, Y. J., Shih, K. C. & Chou, T. C. Fucoidan Prevents RANKL-Stimulated Osteoclastogenesis and LPS-Induced Inflammatory Bone Loss via Regulation of Akt/GSK3beta/PTEN/NFATc1 Signaling Pathway and Calcineurin Activity. *Mar. Drugs* **17**, https://doi.org/10.3390/md17060345 (2019).
24. Liyanage, N. M. et al. Characterization and therapeutic effect of Sargassum coreanum fucoidan that inhibits lipopolysaccharide-induced inflammation in RAW 264.7 macrophages by blocking NF-kappaB signaling. *Int. J. Biol. Macromol.* **223**, 500–510 (2022).
25. Cho, Y. D. et al. Molecular regulation of matrix extracellular phosphoglycoprotein expression by bone morphogenetic protein-2. *J. Biol. Chem.* **284**, 25230–25240 (2009).
26. Pereira, J. et al. The in vitro and in vivo effects of a low-molecular-weight fucoidan on the osteogenic capacity of human adipose-derived stromal cells. *Tissue Eng. Part A* **20**, 275–284 (2014).
27. Jin, X. et al. Low-molecular weight fucoidan inhibits the differentiation of osteoclasts and reduces osteoporosis in ovariectomized rats. *Mol. Med. Rep.* **15**, 890–898 (2017).
28. Hwang, P. A. et al. The in vitro and in vivo effects of the low molecular weight fucoidan on the bone osteogenic differentiation properties. *Cytotechnology* **68**, 1349–1359 (2016).
29. Wang, J. et al. Tectoridin inhibits osteoclastogenesis and bone loss in a murine model of ovariectomy-induced osteoporosis. *Exp. Gerontol.* **140**, 111057 (2020).
30. Eleniste, P. P., Huang, S., Wayakanon, K., Largura, H. W. & Bruzzaniti, A. Osteoblast differentiation and migration are regulated by dynamin GTPase activity. *Int. J. Biochem. Cell Biol.* **46**, 9–18 (2014).
31. Nakashima, K. et al. The novel zinc finger-containing transcription factor osterix is required for osteoblast differentiation and bone formation. *Cell* **108**, 17–29 (2002).
32. Mann, S. N. et al. 17alpha-Estradiol prevents ovariectomy-mediated obesity and bone loss. *Exp. Gerontol.* **142**, 111113 (2020).
33. Kim, Y. W., Baek, S. H., Lee, S. H., Kim, T. H. & Kim, S. Y. Fucoidan, a sulfated polysaccharide, inhibits osteoclast differentiation and function by modulating RANKL signaling. *Int. J. Mol. Sci.* **15**, 18840–18855 (2014).
34. Jeong, Y. T. et al. Osteoprotective effects of Polysaccharide-Enriched Hizikia fusiforme processing byproduct in vitro and in vivo models. *J. Med. Food* **19**, 805–814 (2016).
35. Zhang, R., Zhang, X., Tang, Y. & Mao, J. Composition, isolation, purification and biological activities of *Sargassum fusiforme* polysaccharides: a review. *Carbohydr. Polym.* **228**, 115381 (2020).
36. Savage, P. E. Chemistry. Algae under pressure and in hot water. *Science* **338**, 1039–1040 (2012).
37. Silva, M. et al. Comparison of in vitro and in vivo antioxidant activities of commercial fucoidans from Macrocystis pyrifera, Undaria pinnatifida, and Fucus vesiculosus. *Int. J. Biol. Macromol.* **216**, 757–767 (2022).
38. Kim, K. J., Yoon, K. Y. & Lee, B. Y. Low molecular weight fucoidan from the sporophyll of Undaria pinnatifida suppresses inflammation by promoting the inhibition of mitogen-activated protein kinases and oxidative stress in RAW264.7 cells. *Fitoterapia* **83**, 1628–1635 (2012).
39. Yu, J. et al. Fucoidan extracted from Sporophyll of Undaria pinnatifida Grown in Weihai, China - chemical composition and comparison of antioxidant activity of different molecular weight fractions. *Front. Nutr.* **8**, 636930 (2021).
40. Thuy, T. T. et al. Anti-HIV activity of fucoidans from three brown seaweed species. *Carbohydr. Polym.* **115**, 122–128 (2015).
41. Jin, W. et al. Interactions of fibroblast growth factors with sulfated galactofucan from Saccharina japonica. *Int. J. Biol. Macromol.* **160**, 26–34 (2020).
42. Zhi, X. et al. l-tetrahydropalmatine suppresses osteoclastogenesis in vivo and in vitro via blocking RANK-TRAF6 interactions and inhibiting NF-kappaB and MAPK pathways. *J. Cell Mol. Med.* **24**, 785–798 (2020).
43. Wang, Q. et al. Madecassoside inhibits estrogen deficiency-induced osteoporosis by suppressing RANKL-induced osteoclastogenesis. *J. Cell Mol. Med.* **23**, 380–394 (2019).
44. Bernar, A., Gebetsberger, J. V., Bauer, M., Streif, W. & Schirmer, M. Optimization of the Alizarin Red S Assay by Enhancing Mineralization of Osteoblasts. *Int. J. Mol. Sci.* **24**, https://doi.org/10.3390/ijms24010723 (2022).
45. Kiyomiya, H. et al. IL-33 inhibits RANKL-induced osteoclast formation through the regulation of Blimp-1 and IRF-8 expression. *Biochem. Biophys. Res. Commun.* **460**, 320–326 (2015).
46. Zhao, R. et al. Melatonin rescues glucocorticoid-induced inhibition of osteoblast differentiation in MC3T3-E1 cells via the PI3K/AKT and BMP/Smad signalling pathways. *Life Sci.* **257**, 118044 (2020).
47. Tang, Y., Lv, X. L., Bao, Y. Z. & Wang, J. R. Glycyrrhizin improves bone metabolism in ovariectomized mice via inactivating NF-kappaB signaling. *Climacteric* **24**, 253–260 (2021).
48. Liu, X. et al. The beneficial effect of Praeruptorin C on osteoporotic bone in ovariectomized mice via suppression of osteoclast formation and bone resorption. *Front. Pharmacol.* **8**, 627 (2017).
49. Zhu, K. et al. Sulfated Galactofucan from Sargassum Thunbergii Attenuates Atherosclerosis by suppressing inflammation via the TLR4/MyD88/NF-kappaB Signaling Pathway. *Cardiovasc. Drugs Ther.* **38**, 69–78 (2024).
50. Liu, Y., Wu, X., Wang, Y., Jin, W. & Guo, Y. The immunoenhancement effects of starfish Asterias rollestoni polysaccharides in macrophages and cyclophosphamide-induced immunosuppression mouse models. *Food Funct.* **11**, 10700–10708 (2020).


## Acknowledgements

This study was supported by National Natural Science Foundation of China (No. 81801397).

## Author contributions

Yizhong Bao: Conceptualization, Investigation, Project administration, Funding acquisition. Fen Chen: Conceptualization, Methodology, Writing-original draft. Weihua Jin: Conceptualization, Resources, Methodology, Writing-review & editing. Jihuan Dai: Methodology, Investigation, Project administration. Genxiang Mao: Methodology, Formal analysis. Boshan Song: Conceptualization, Investigation, Funding acquisition.

## Competing interests

The authors declare no competing interests.

## Additional information

**Supplementary information** The online version contains supplementary material available at https://doi.org/10.1038/s42003-024-07097-2.

**Correspondence** and requests for materials should be addressed to Genxiang Mao or Boshan Song.

**Peer review information** *Communications Biology* thanks Dhanak Gupta, Gwendolen Reilly, and the other, anonymous, reviewer for their contribution to the peer review of this work. Primary Handling Editors: Joao Valente.